

# **β-delayed neutron spectroscopy of $^{85,86}\text{As}$ with MONSTER**

**A. Pérez de Rada, V. Alcayne, D. Cano-Ott, T. Martínez, E. Mendoza, J. Plaza, A. Sanchez-Caballero,  
D. Villamarín (CIEMAT)**

J. Äystö, A. Jokinen, A. Kankainen, H. Penttilä, S. Rinta-Antila (JYFL)

J. Agramunt, A. Algora, C. Domingo-Pardo, J. Lerendegui-Marco, J.L. Taín (IFIC)

K. Banerjee, C. Bhattacharya, P. Roy (VECC)

F. Calviño, G. Cortés (UPC)

C. Delafosse, I. Matea (IJCLab)

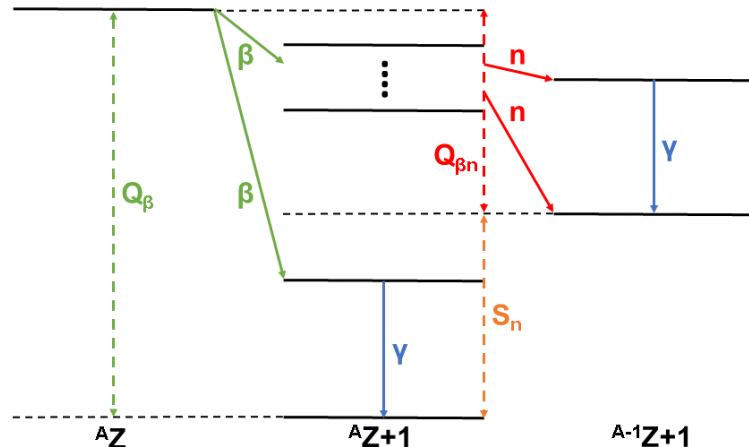
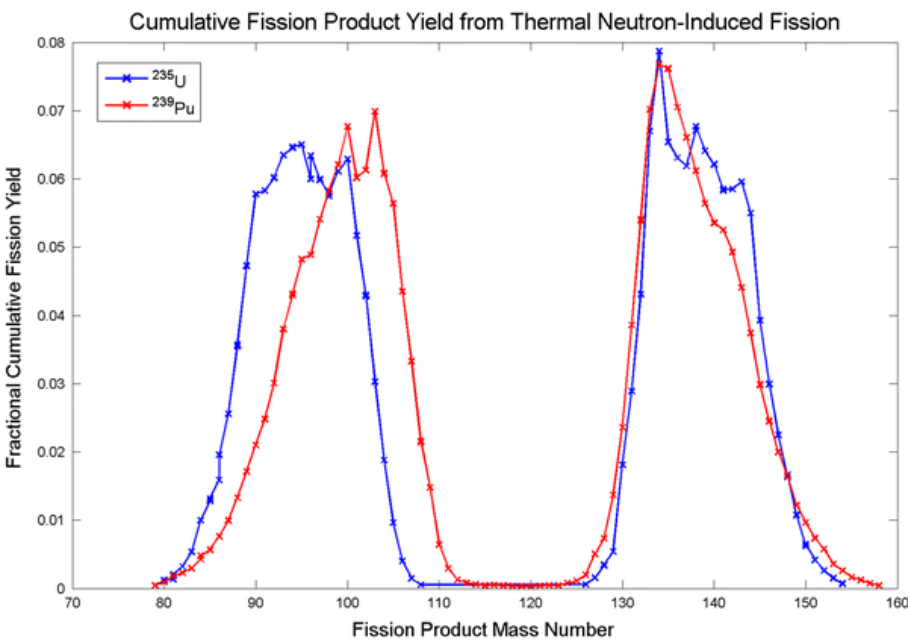
J. Benito (UCM)



# Physics case

$\beta$ -delayed neutrons are interesting for:

- Nuclear structure
- Nuclear astrophysics
- Fission reactor kinetics and control



Priority list for reactor studies:

$^{86}\text{Ge}$ ,  $^{85,86}\text{As}$ ,  $^{91}\text{Br}$ ,  $^{93}\text{Rb}$ ,  $^{98\text{m}},^{98}\text{Y}$ ,  $^{135}\text{Sb}$ ,  
 $^{139}\text{I}$ ,  $^{88}\text{As}$ ,  $^{96}\text{Rb}$ ,  $^{105,106}\text{Nb}$ ,  $^{137}\text{Sb}$ ,  $^{136}\text{Te}$ ,  
 $^{140}\text{I}$ ,  $^{143,144}\text{Cs}$

INDC(NDS)-0643

- M. B. Gomez-Hornillos *et al.*, Hyperfine Interactions, **223**, (2014) 185  
J. Agramunt *et al.*, Nuclear Data Sheets, **120**, (2014) 74-77  
J. Agramunt *et al.*, Nucl. Instrum. and Methods A, **807**, (2016) 69  
R. Caballero-Folch *et al.*, Nuclear Data Sheets, **120**, (2014) 81-83  
R. Caballero-Folch *et al.*, Physical Review Letters, **117**, (2016) 012501  
R. Caballero-Folch *et al.*, Physical Review C, **95**, (2017) 064322  
A. R. Garcia, PhD Thesis (2020)



# MONSTER

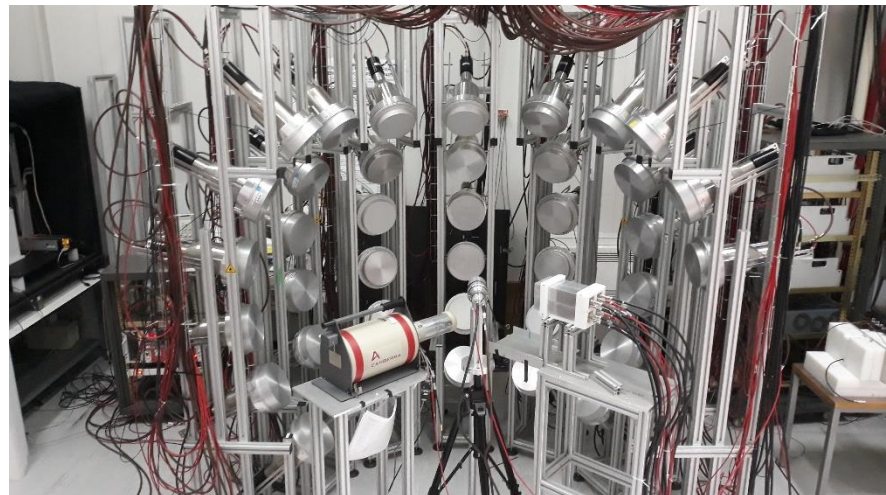
**MO**dular **N**eutron time-of-flight **S**pectrome**T**ER

International collaboration between CIEMAT, JYFL,  
VECC, IFIC, and UPC

Consists of 65 cells of liquid scintillator (up to 100)

Main characteristics:

- Low energy threshold
- High intrinsic neutron detection efficiency
- Detects both  $\gamma$ -rays and neutrons
  - Discriminates between them by the pulse shape
- Good time resolution
- The energy of the neutrons is determined with the time-of-flight technique
- For this experiment, 48 cells were used (CIEMAT + JYFL)



A.R. Garcia *et al.*, JINST, **7**, (2012) C05012

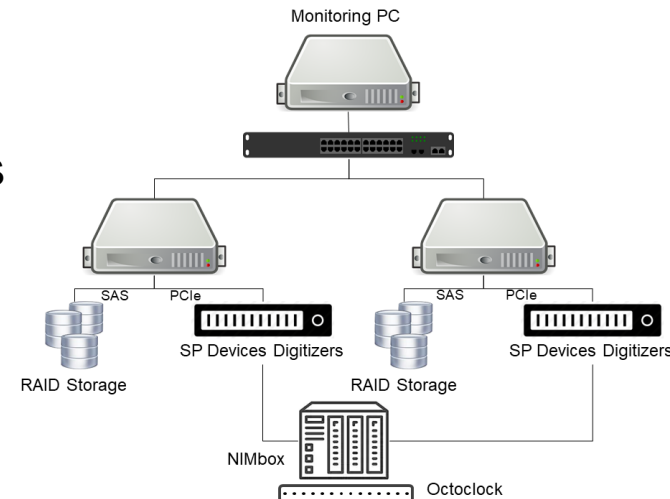
T. Martinez *et al.*, Nuclear Data Sheets, **120**, (2014) 78

# Digital data Acquisition System (DAISY)

Custom DAQ software developed at CIEMAT

## Hardware:

- 15 ADQ14 SP Devices cards (14bits, 1GS/s)
- 2 Counter/Timer PCIe6612 National Instruments
- NI Octoclock CDA-2990 (10MHz, 8 ch)
- Wiener NIM/TTL Programmable modules
- 2 PCs + 2 PCIe crates
- 3 96 TB RAID 6



D. Villamarin *et al.*, in preparation



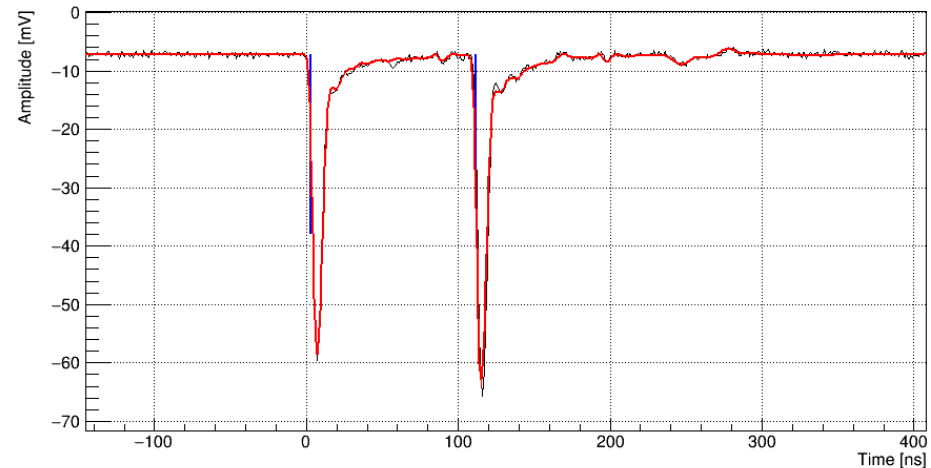
# Pulse shape analysis software

β-detector

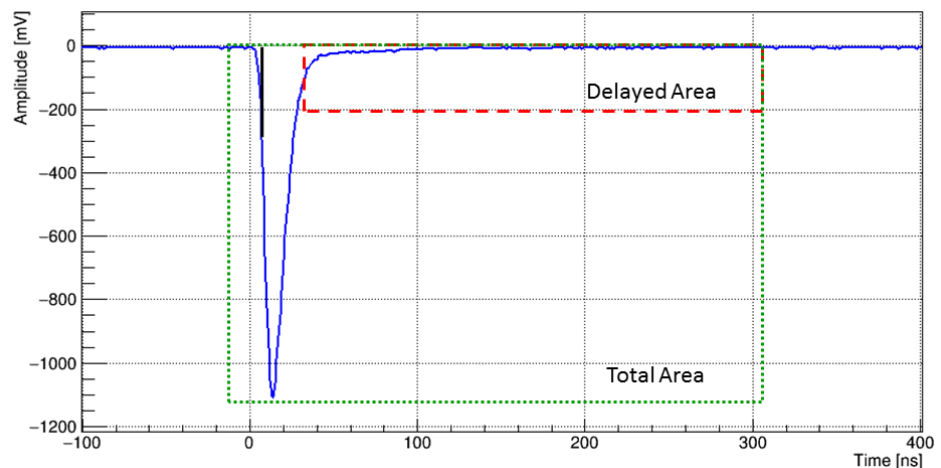
Developed at CIEMAT

Analyzes signals on-line:

- With several available routines:
  - Digital integration in regions
  - Fit to the average signal
- Resolving pile-ups
- Without adding a dead time



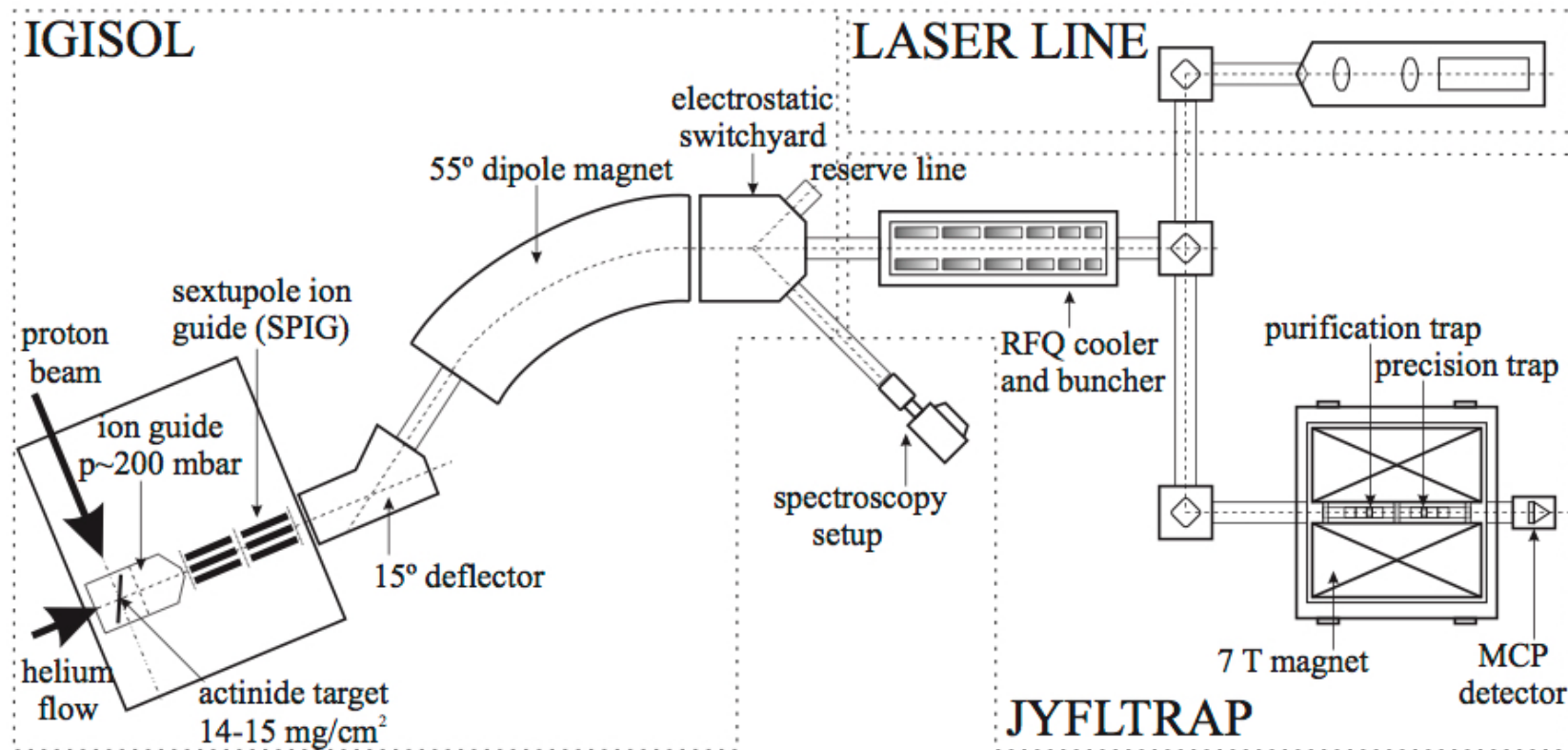
MONSTER



# The Accelerator Laboratory of the University of Jyväskylä (JYFL)

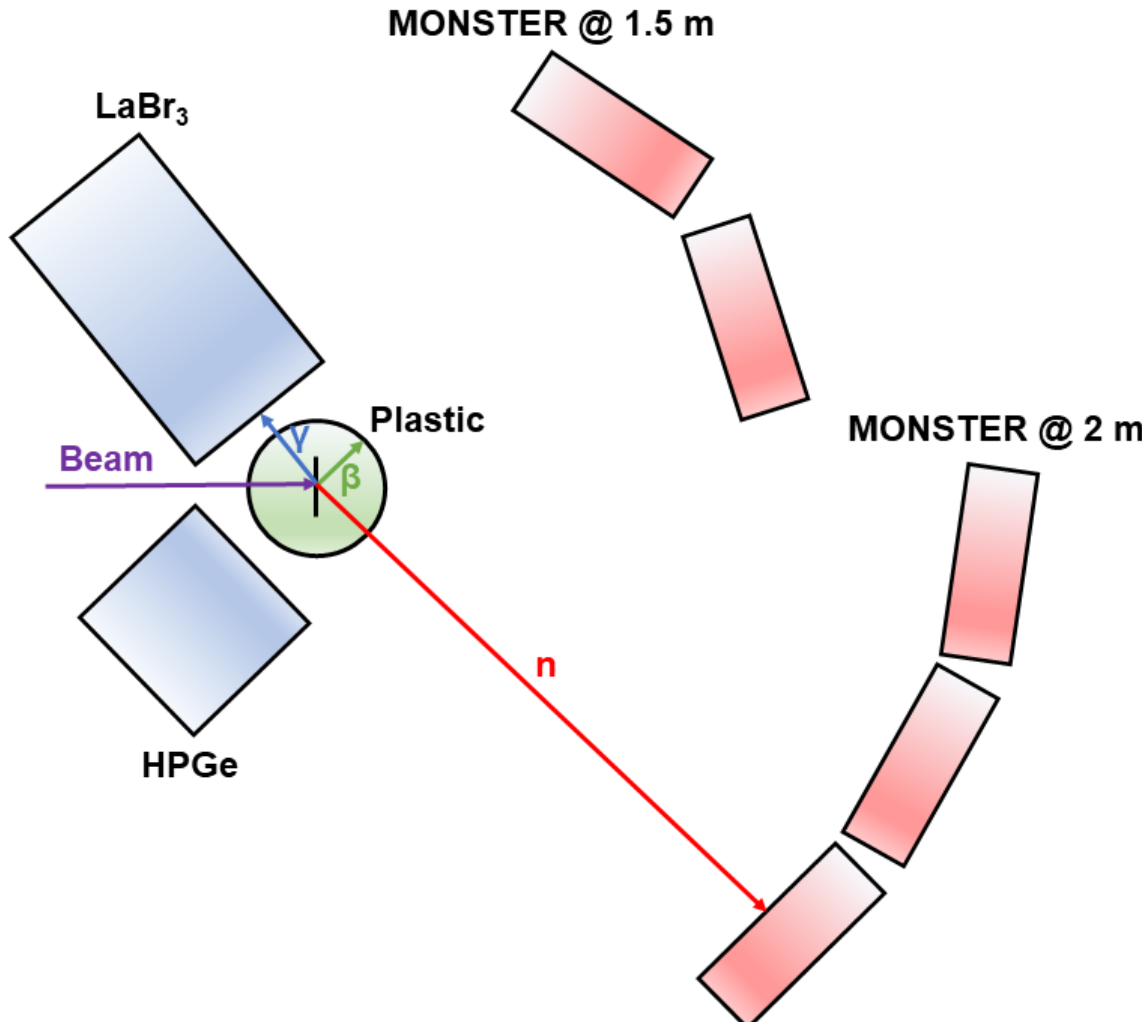
Located in Jyväskyla, Finland

IGISOL → Ion Guide Isotope Separation OnLine

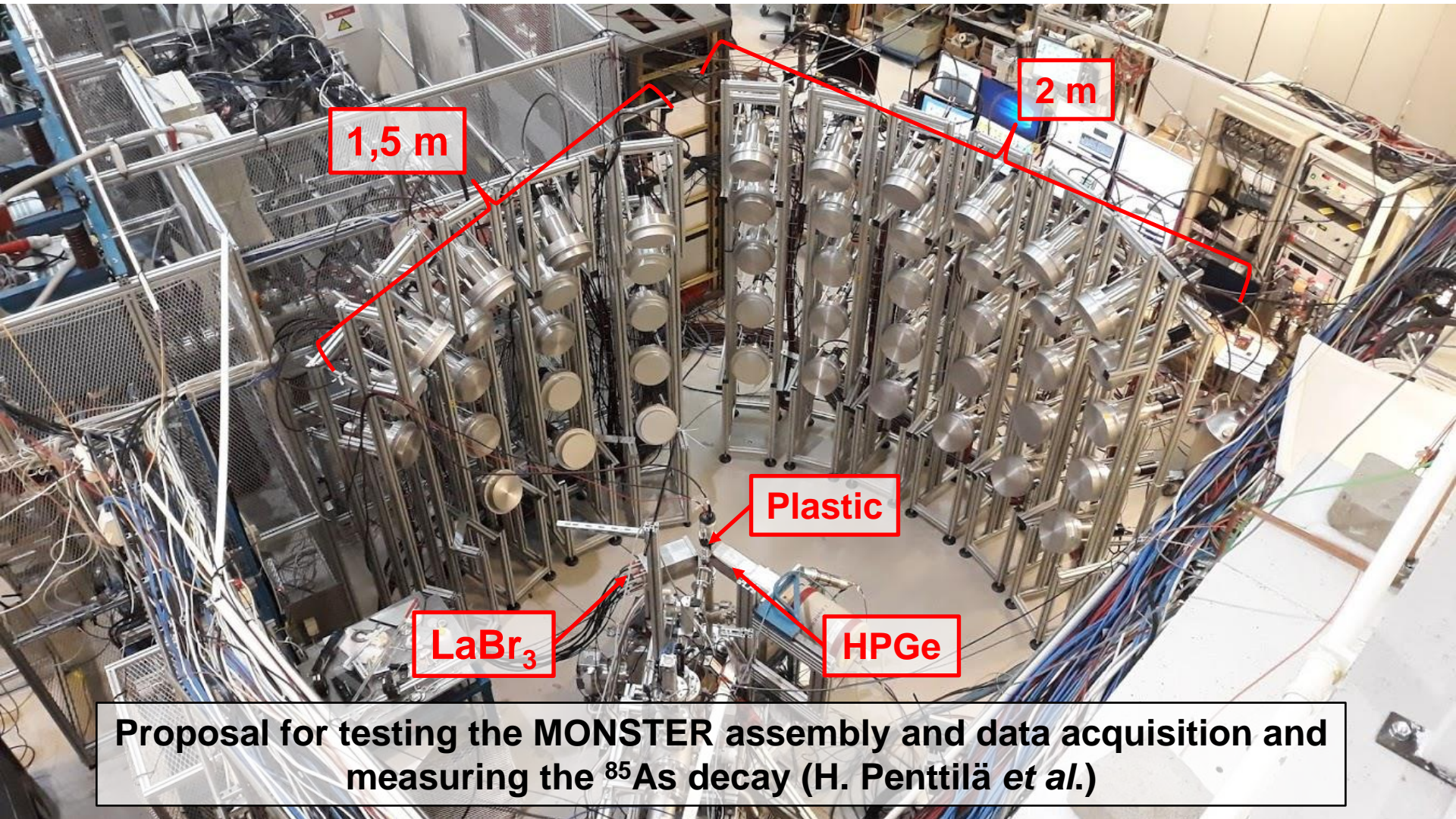


I. D. Moore *et al.*, Nucl. Instrum. and Methods B, 317, (2013) 208

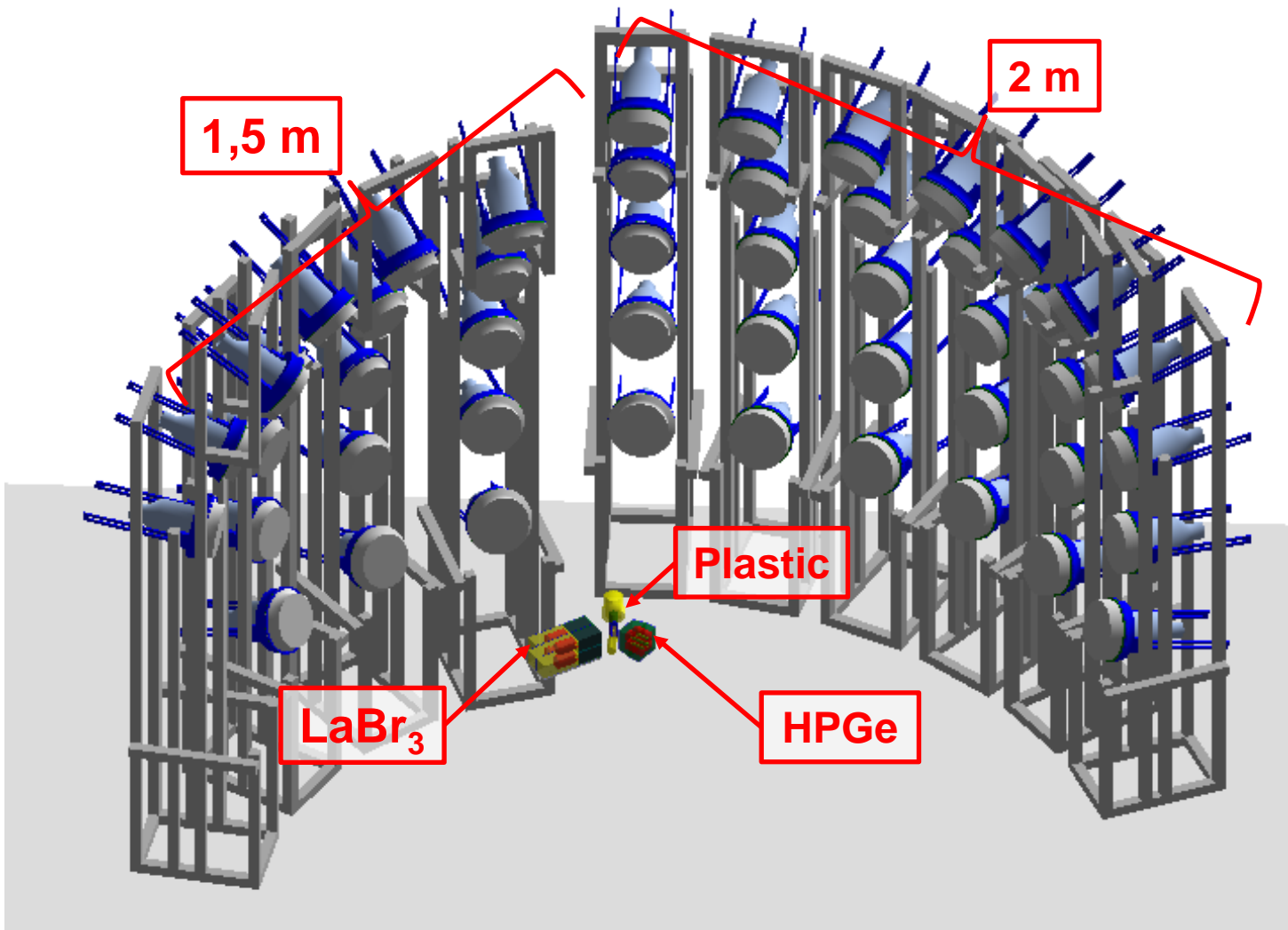
# MONSTER setup @ JYFL



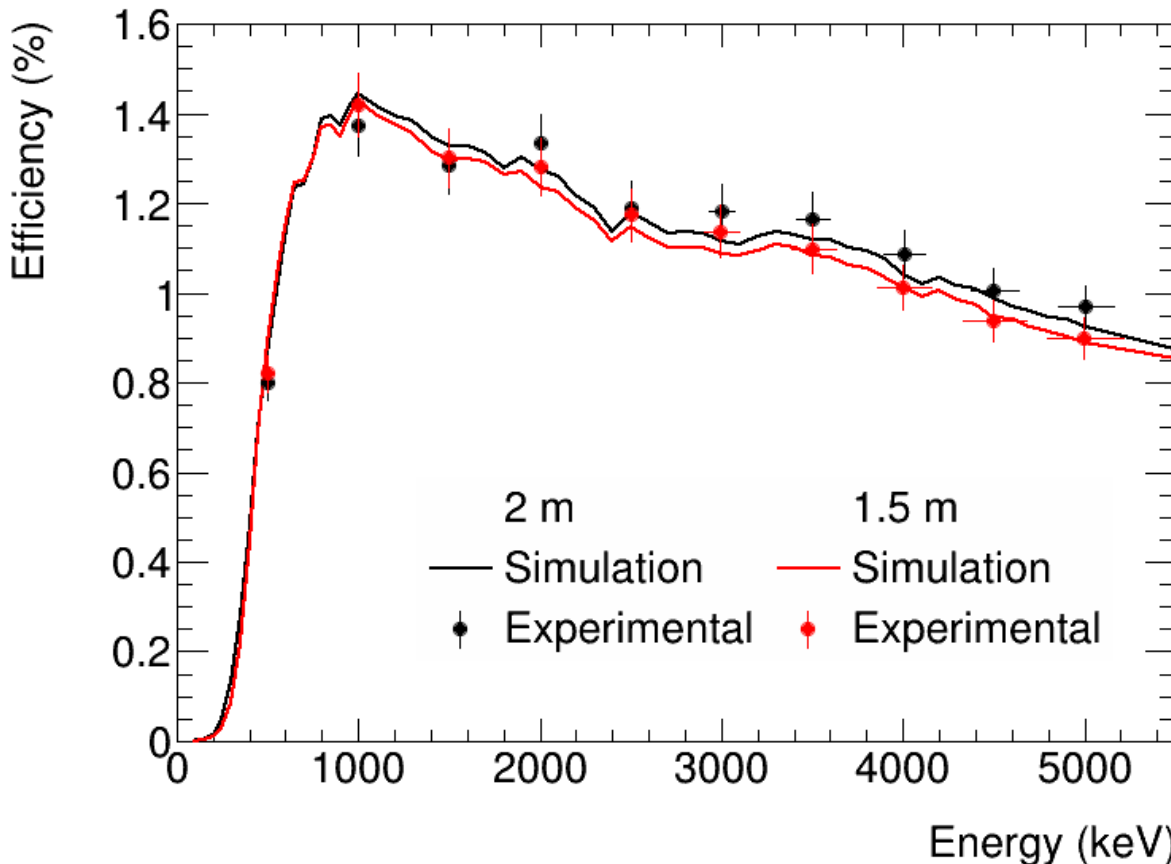
# MONSTER setup @ JYFL



# MONSTER setup @ JYFL



# Neutron detection efficiency

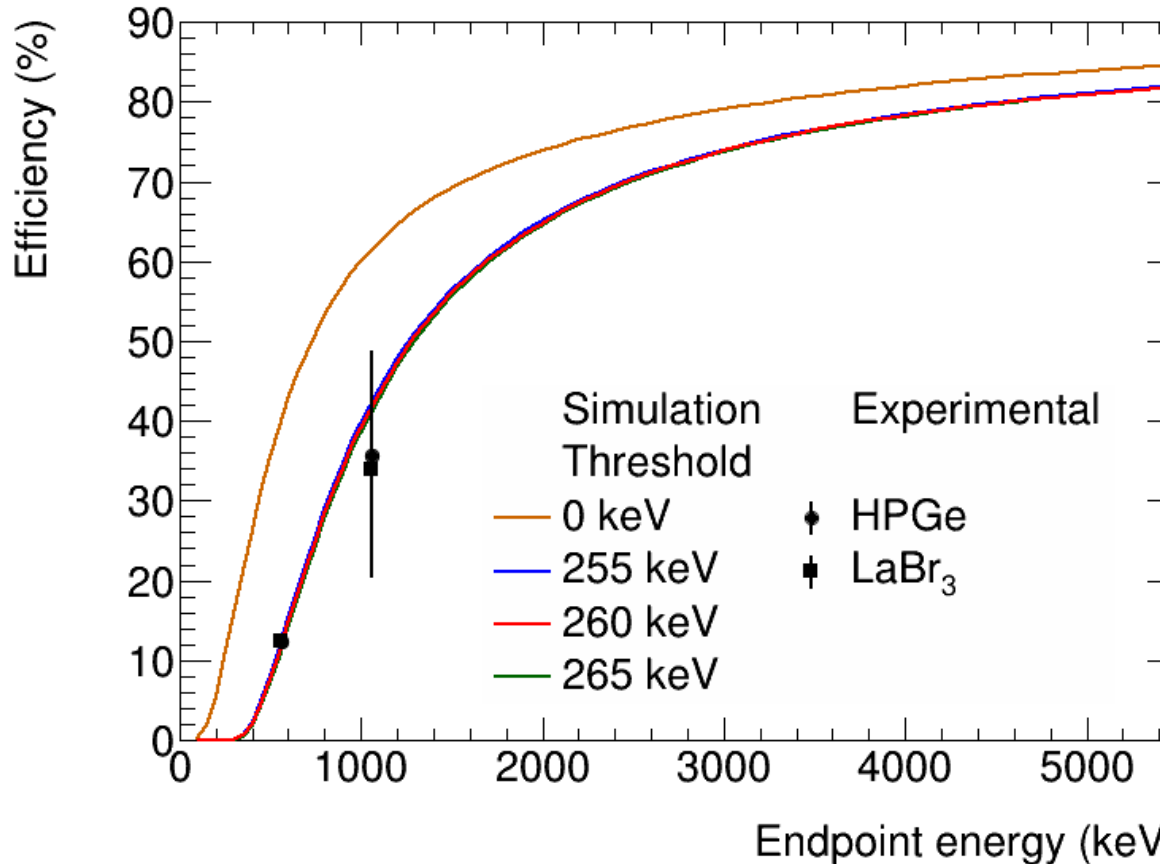


Accurate Monte Carlo simulations calibrated at PTB and in-situ calibration with a  $^{252}\text{Cf}$  neutron source.

A. R. Garcia *et al.*, Nucl. Instrum. and Methods A, **868**, (2017) 73-81

# $\beta$ -detection efficiency

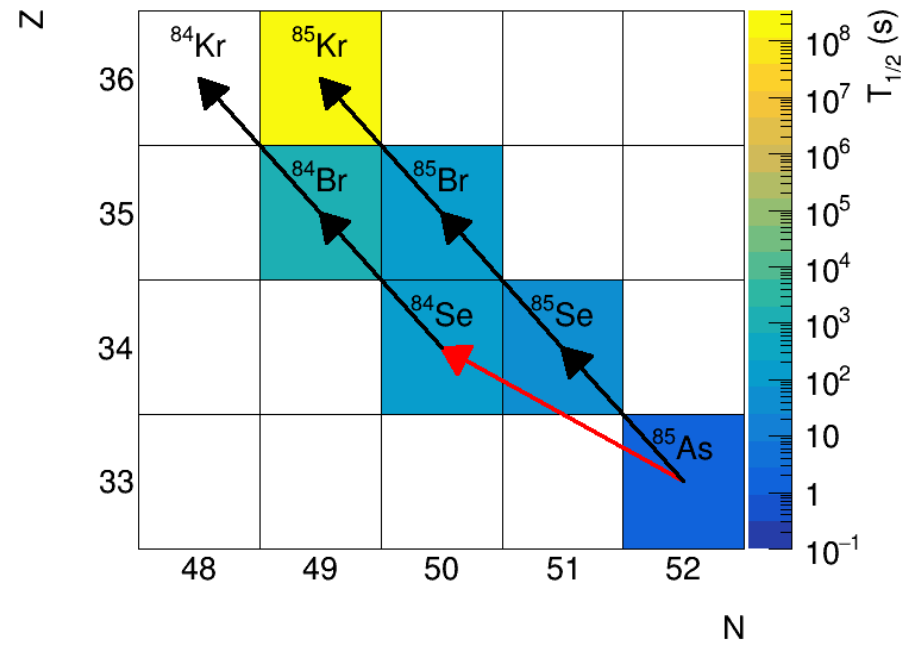
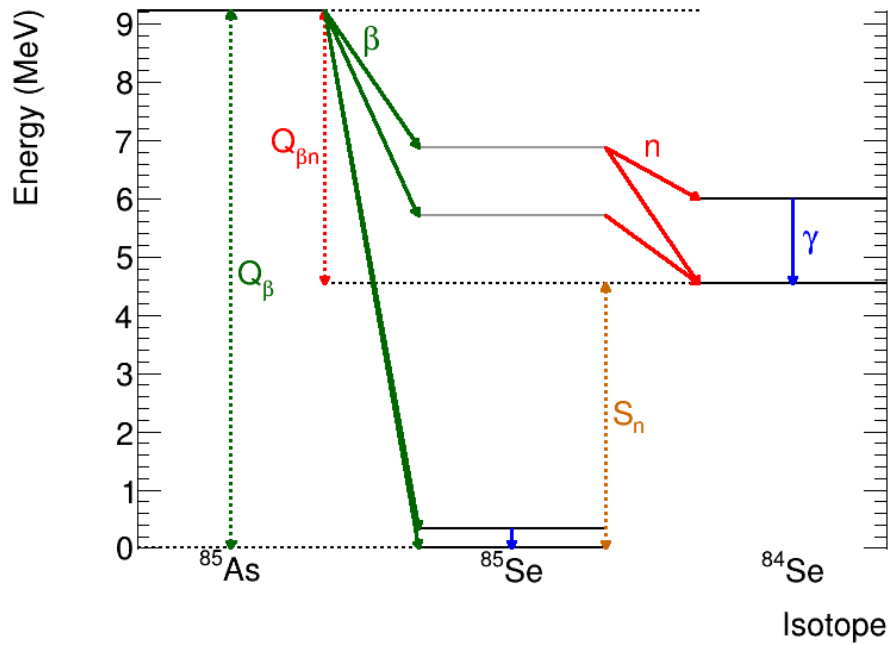
The  $\beta$ -detection efficiency depends on the  $\beta$ -detector threshold and varies up to the  $Q_\beta$ .



The efficiency for all the decays was obtained by detailed Monte Carlo simulations of the decays and validated with data from <sup>92</sup>Sr into <sup>92</sup>Y.



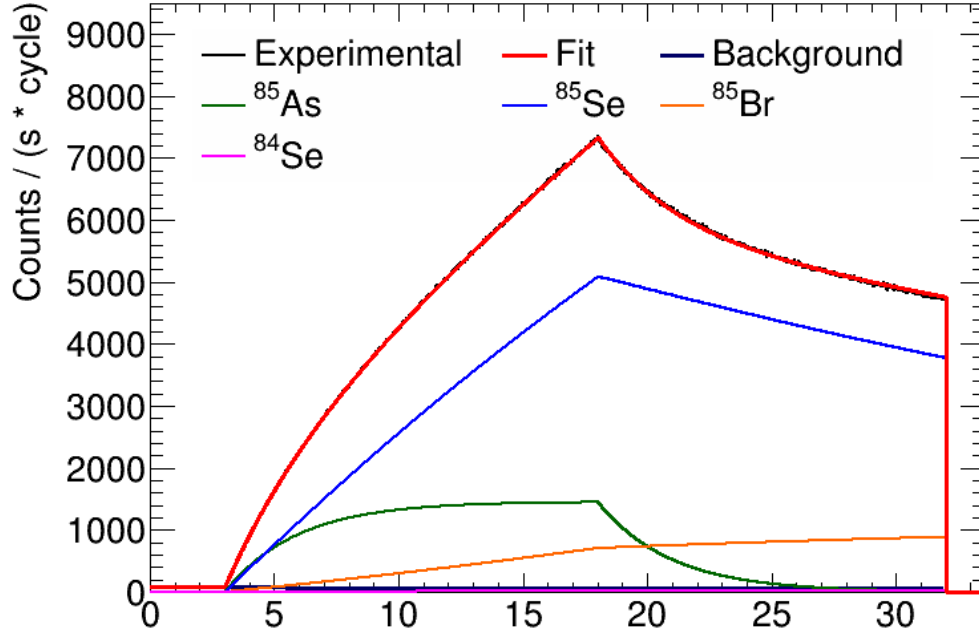
# $^{85}\text{As}$ $\beta$ -decay



$$P_n = 59.4 \pm 2.4 \%$$

D. A. Brown *et al.*, Nucl. Data Sheets, **148**, (2018) 1-142

# Solving the Bateman equations: $^{85}\text{As}$



$^A\text{Z}$	$\bar{\epsilon} (\%)$	$R (\text{nuclei/s})$	Decays
$^{85}\text{As}$	80.8	1800	$4.8 \times 10^7$
$^{85}\text{Se}$	76.0	23300	$2.39 \times 10^8$
$^{85}\text{Br}$	69.7	13900	$4.2 \times 10^7$
$^{84}\text{Se}$	55.1	0	$1.8 \times 10^6$

$$N_n(t) = \sum_{i=1}^n N_i(t_0) \left( \prod_{j=i}^{n-1} (\lambda_j b_{j,j+1}) \sum_{j=i}^n \frac{e^{-\lambda_j(t-t_0)}}{\prod_{p=i, p \neq j}^n (\lambda_p - \lambda_j)} \right)$$

$$+ \sum_{i=1}^n R_i \left( \prod_{j=i}^{n-1} (\lambda_j b_{j,j+1}) \sum_{j=i}^n \frac{1 - e^{-\lambda_j(t-t_0)}}{\lambda_j \prod_{p=i, p \neq j}^n (\lambda_p - \lambda_j)} \right)$$

Time (s)

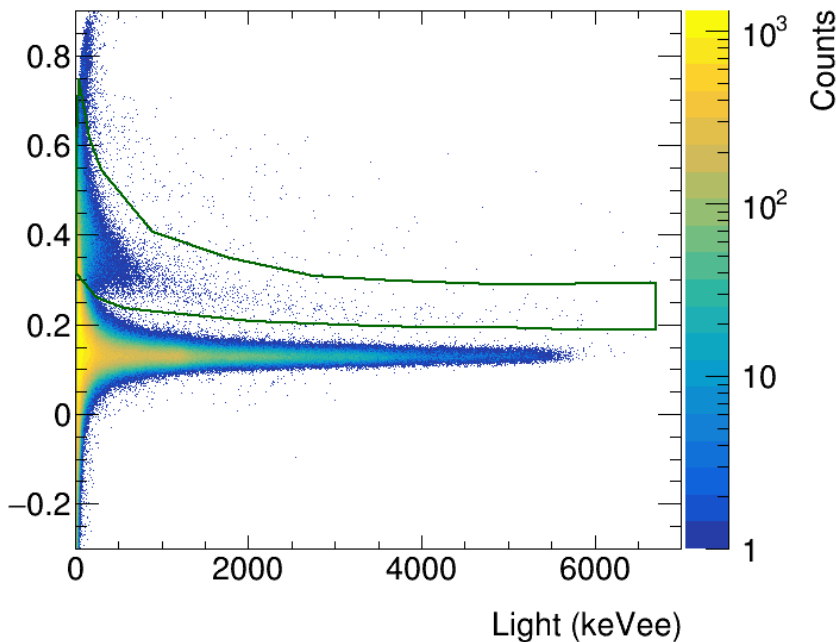
$\rightarrow A(t) = \sum_{i=1}^n \bar{\epsilon}_i \lambda_i N_i(t)$

K. Skrable et al., Health Physics, 27, (1974) 155-157

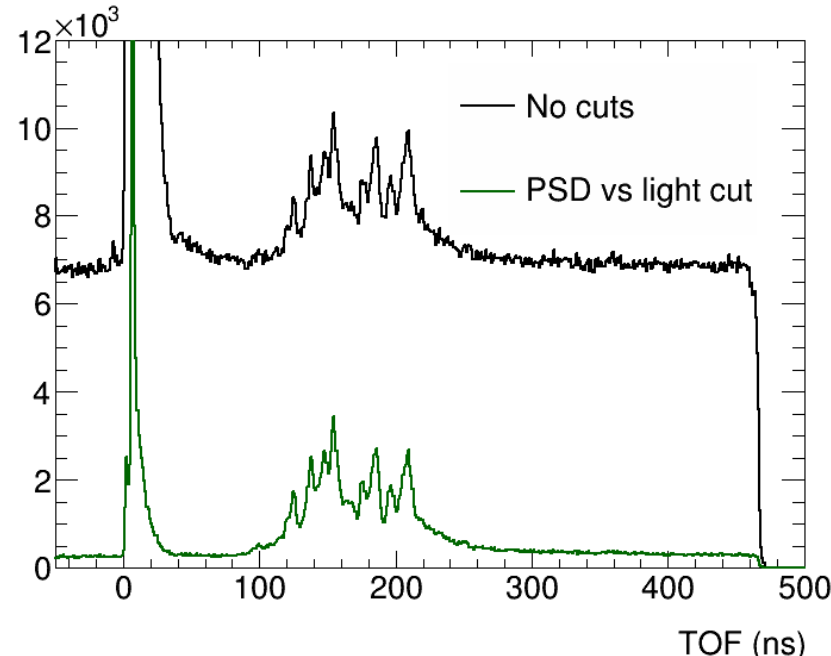
# Analysis of the $^{85}\text{As}$ neutron TOF data

PSD vs light cut applied to obtain a “clean” neutron TOF spectrum.

PSD



Counts



More than one order of magnitude of  $\gamma$ -rays background suppression



GOBIERNO  
DE ESPAÑA

MINISTERIO  
DE CIENCIA  
E INNOVACIÓN

**Ciemat**  
Centro de Investigaciones  
Energéticas, Medioambientales  
y Tecnológicas

EuNPC2022

14

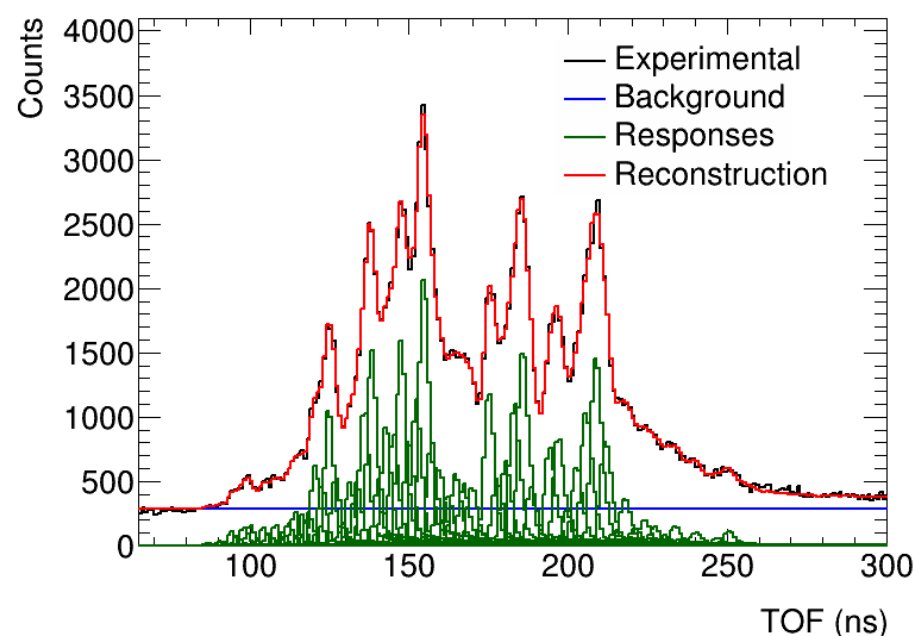
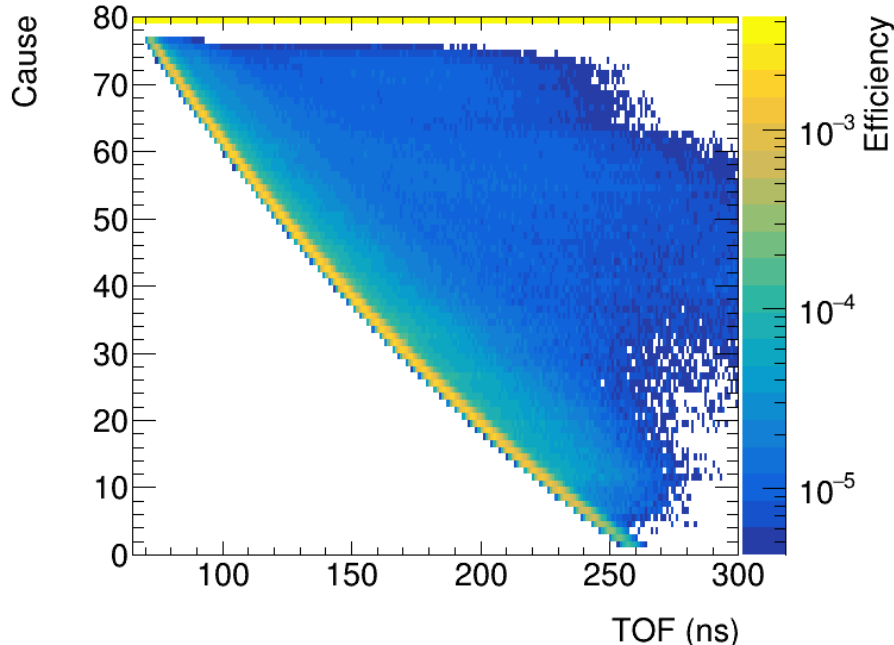
# $^{85}\text{As}$ neutron TOF data unfolding

Unfolding applying an iterative Bayesian method: neutron energy spectrum and  $P_n$  value (with number of decays from the  $\beta$ -activity fit.)

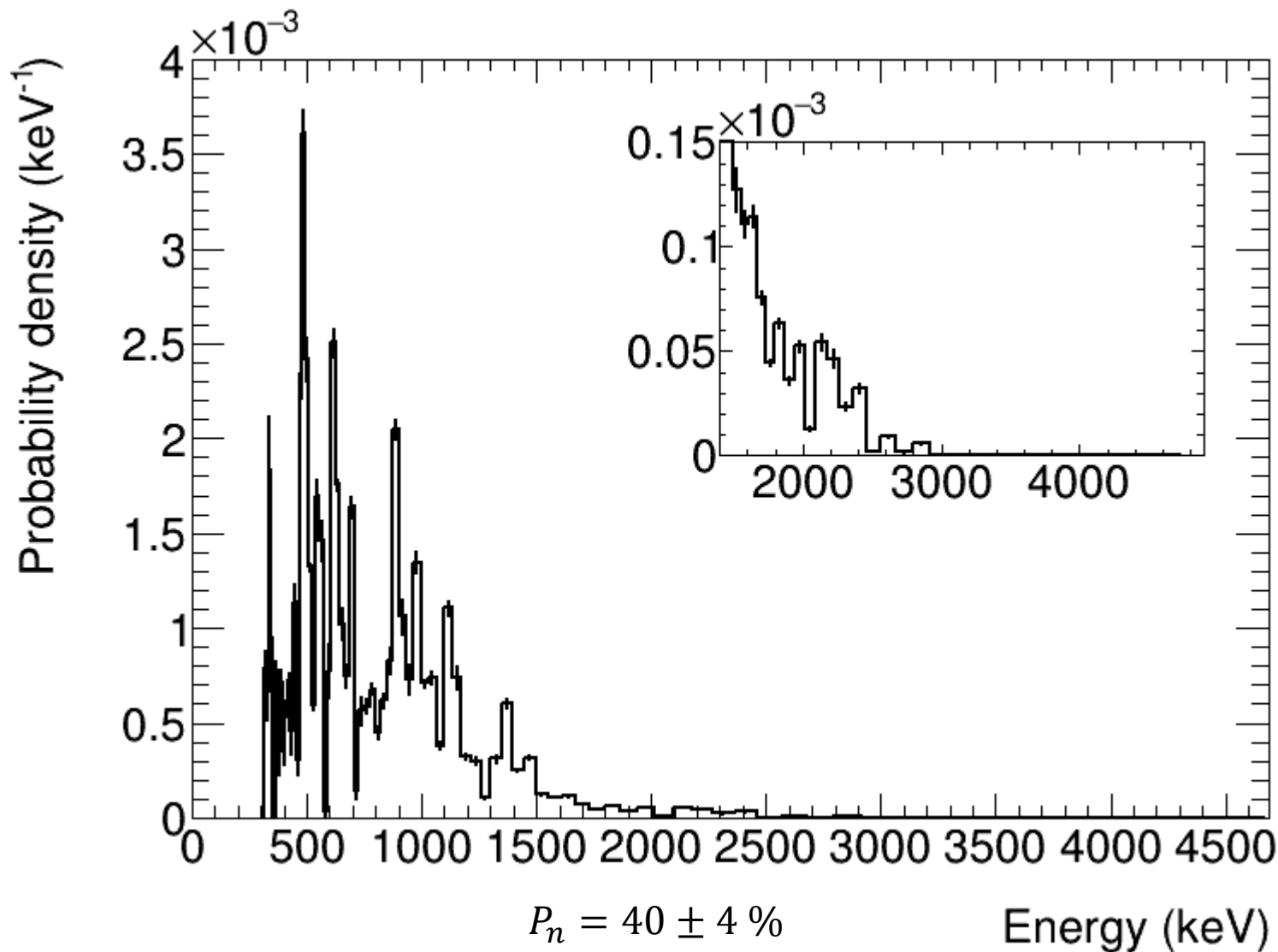
G. D'Agostini., Nucl. Instrum. and Methods A, 362, (1995) 487-498

Response matrix including the light yield, threshold, and time resolution.

$$\frac{\Delta E}{E} = \gamma(\gamma + 1) \sqrt{\left(\frac{\Delta t}{t}\right)^2 + \left(\frac{\Delta L}{L}\right)^2}$$

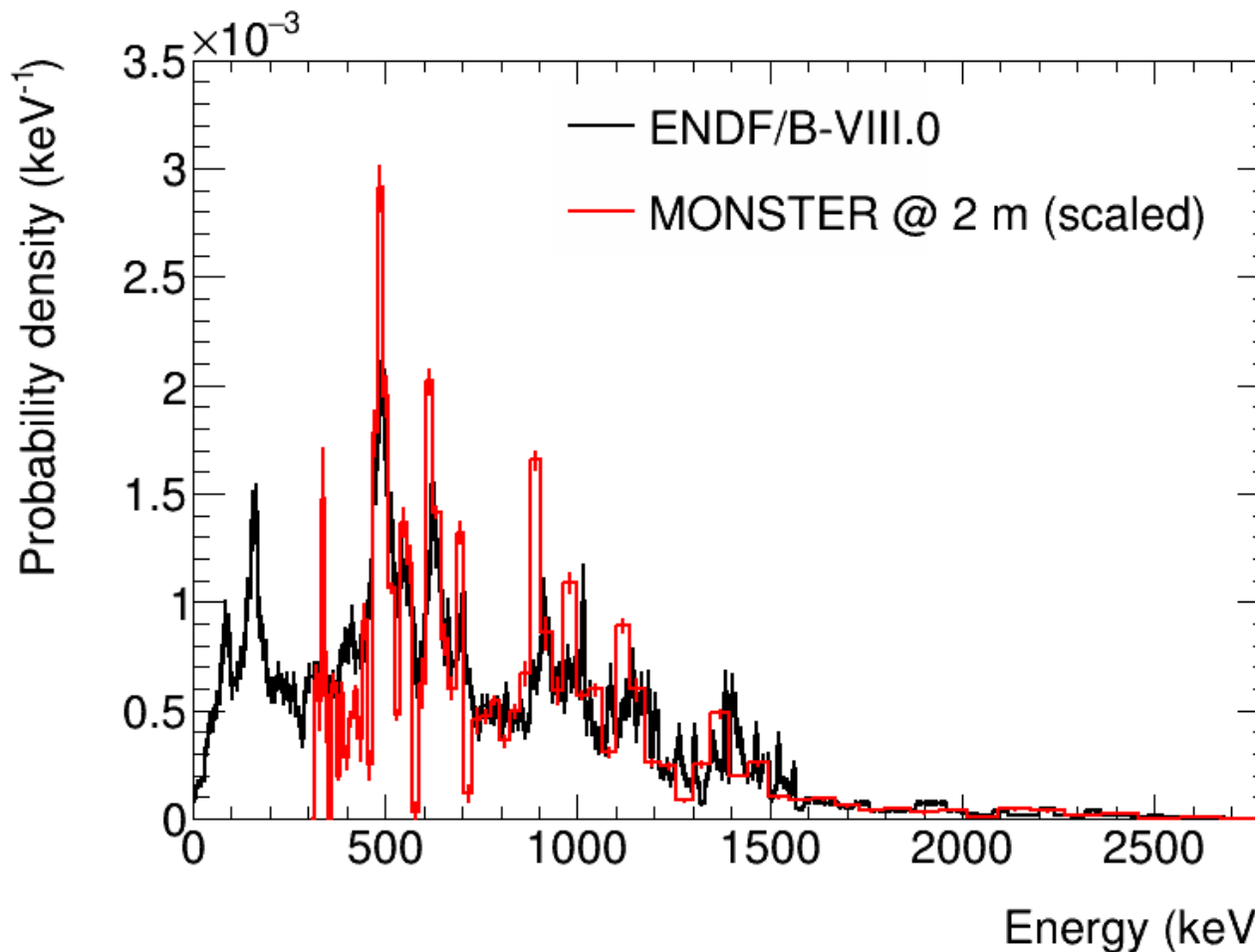


# $^{85}\text{As}$



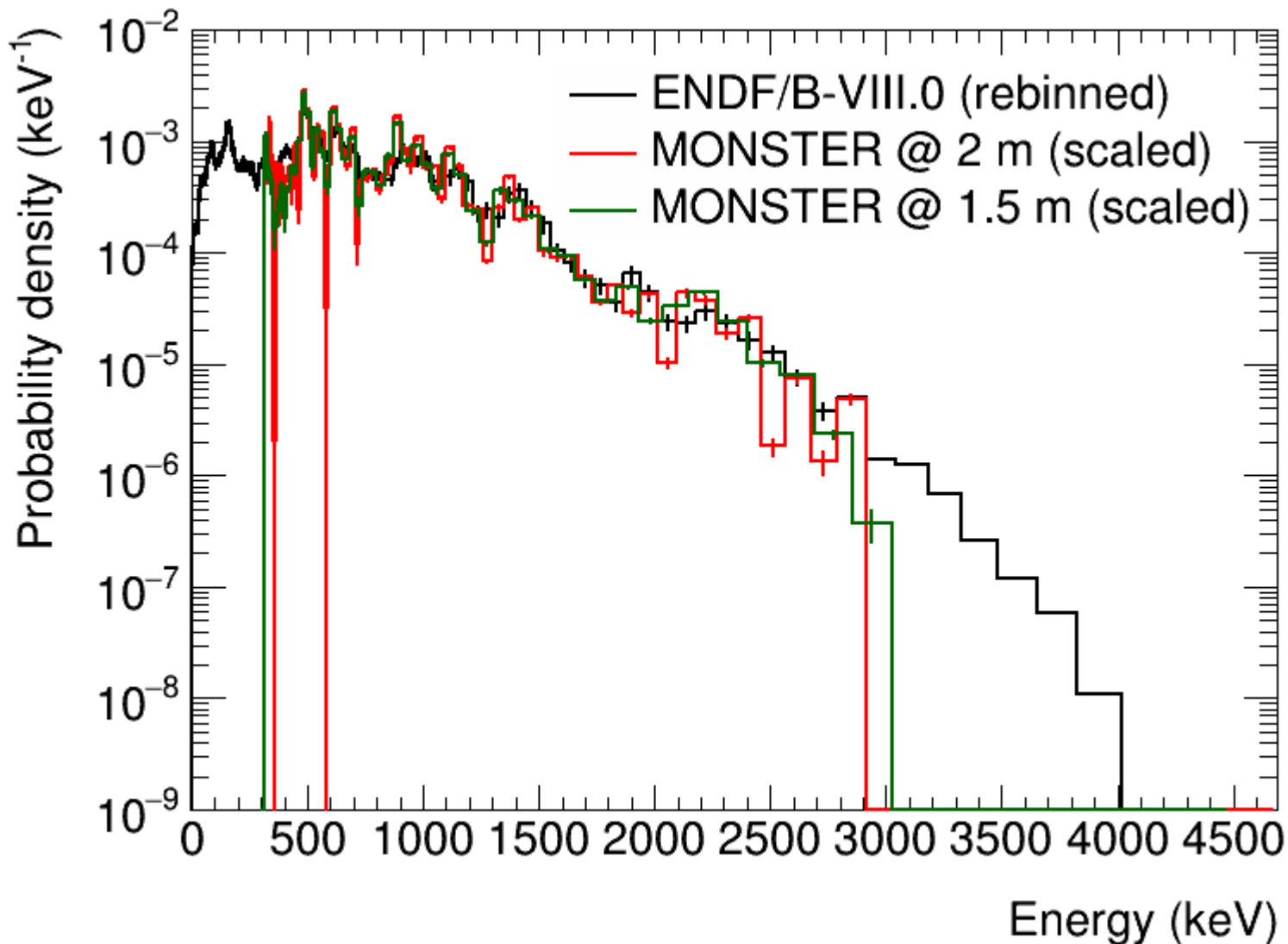
# Comparison of $^{85}\text{As}$ data

Comparison between the MONSTER neutron energy spectrum and previous data.

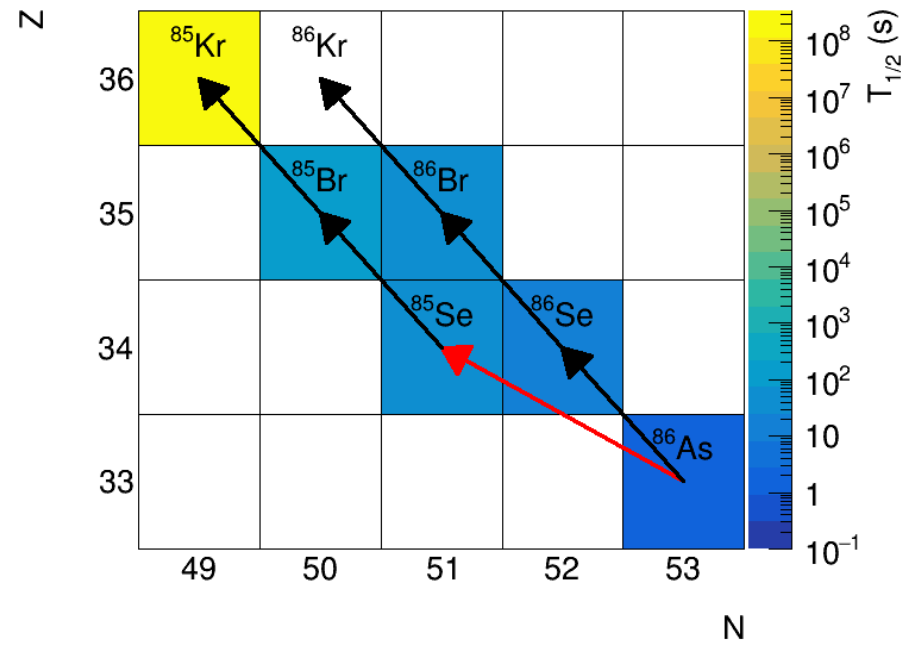
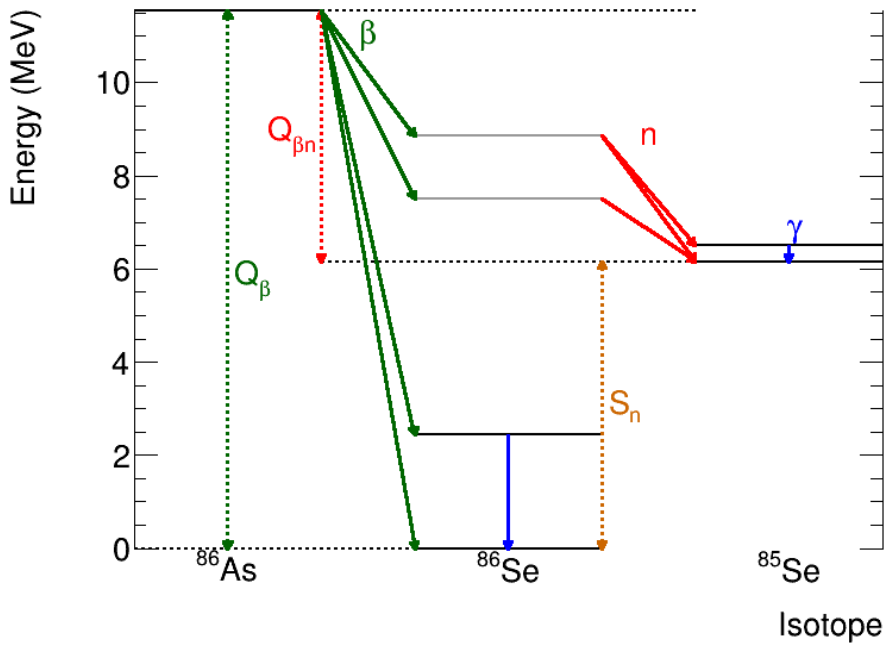


K.-L. Kratz *et al.*, Nucl. Phys. A, 317, (1979) 335

# Final results of $^{85}\text{As}$

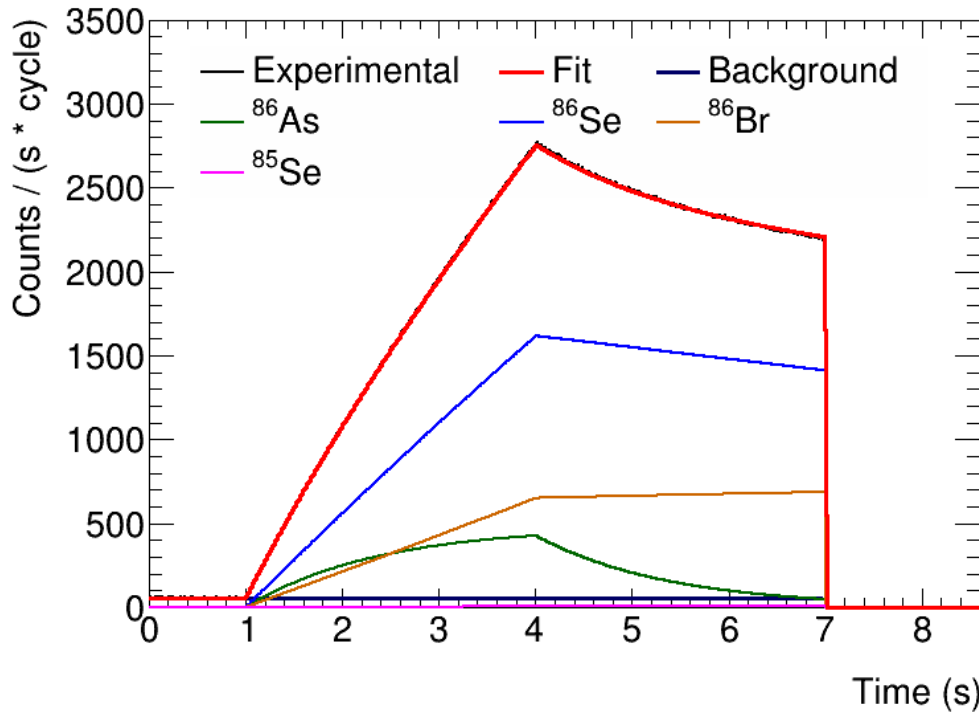


# $^{86}\text{As}$ $\beta$ -decay



$$P_n = 35.5 \pm 0.6 \%$$

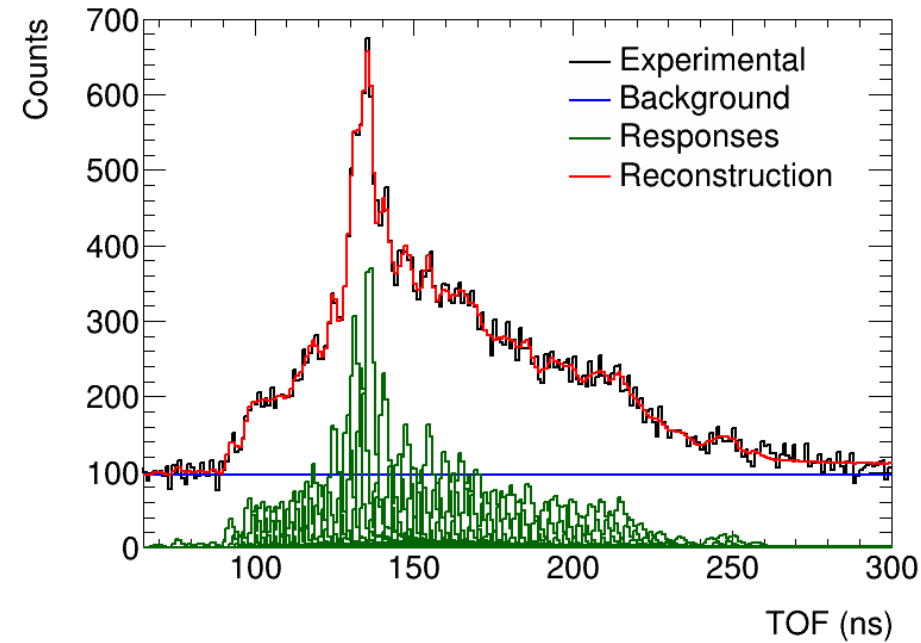
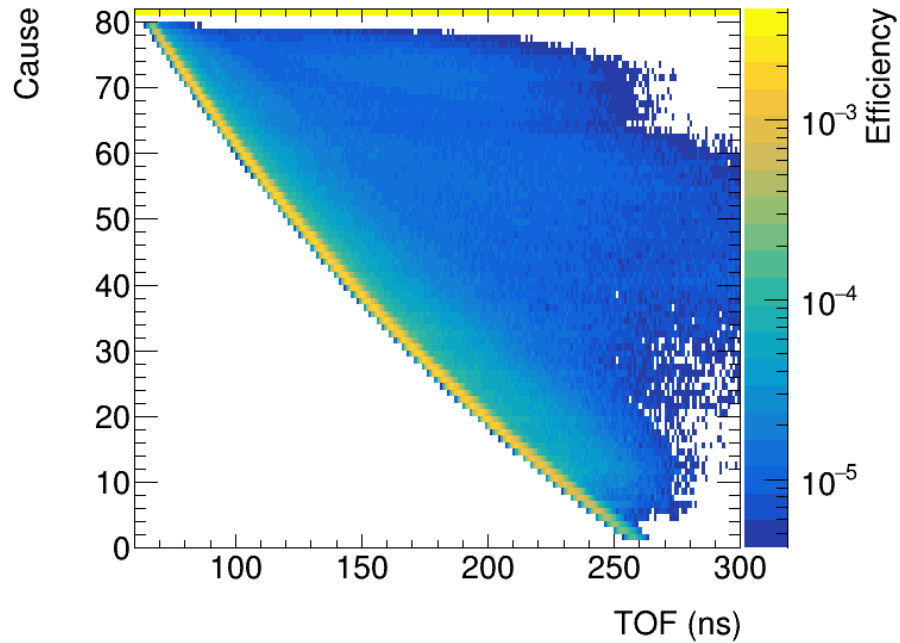
# Solving the Bateman equations: $^{86}\text{As}$



$^A\text{Z}$	$\bar{\epsilon}$ (%)	$R$ (nuclei/s)	Decays
$^{86}\text{As}$	83.5	570	$1.27 \times 10^7$
$^{86}\text{Se}$	72.9	16100	$7.4 \times 10^7$
$^{86}\text{Br}$	77.5	21500	$3.0 \times 10^7$
$^{85}\text{Se}$	76.0	0	$3.2 \times 10^5$

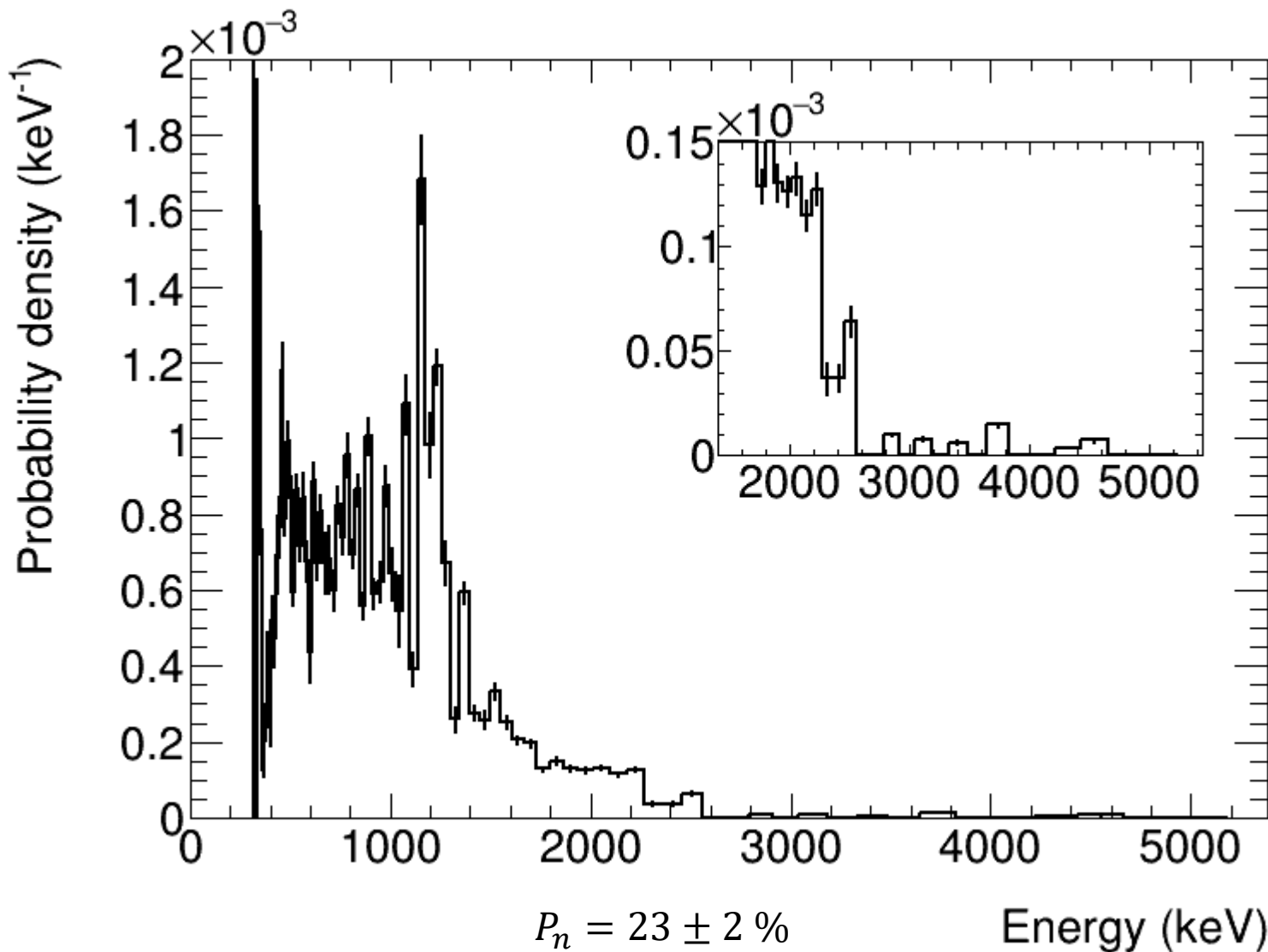
Implantation cycle changed to maximize the contribution of  $^{86}\text{As}$

# $^{86}\text{As}$ neutron TOF data unfolding



Response matrix covers a larger energy range.

# $^{86}\text{As}$



GOBIERNO  
DE ESPAÑA

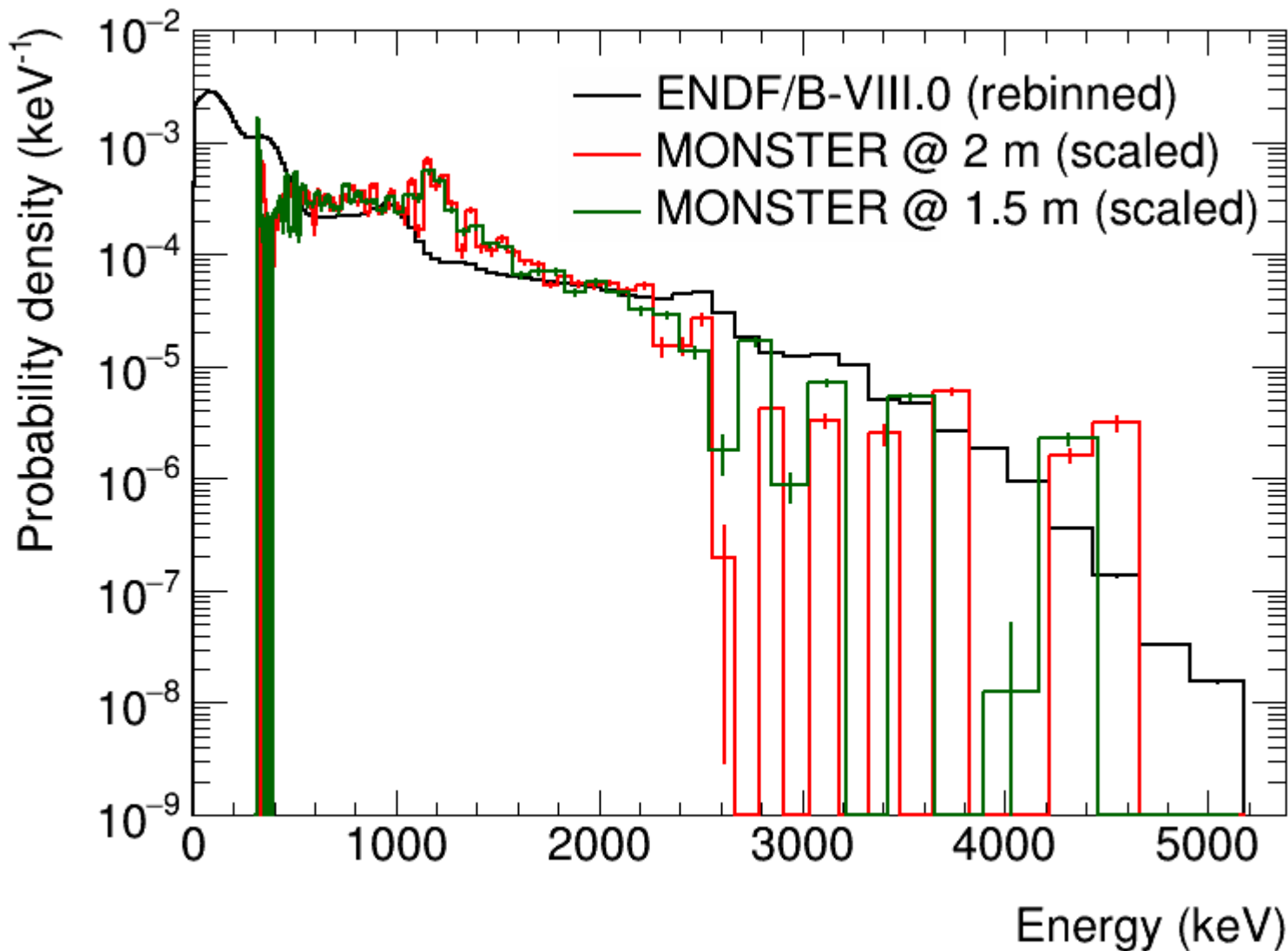
MINISTERIO  
DE CIENCIA  
E INNOVACIÓN

**Ciemat**  
Centro de Investigaciones  
Energéticas, Medioambientales  
y Tecnológicas

EuNPC2022

22

# Final results of $^{86}\text{As}$



# Summary and conclusions

The main takeaways from this work are:

- Successful commissioning and measurement with MONSTER:
  - Good neutron/ $\gamma$ -ray discrimination capabilities.
  - Excellent energy resolution.
- Accurate Monte Carlo simulation of the complete detection system and validation:
  - Reproducing the efficiency of the different detectors (neutrons,  $\gamma$ -rays and  $\beta$ -particles) with known sources, reactions, and decays.
- Analysis methodology:
  - Fit of the  $\beta$ -activity curve with the Bateman equations.
  - Deconvolution of the TOF spectrum with the iterative Bayesian unfolding method.
- Procurement of the neutron energy spectrum of  $^{85}\text{As}$ :
  - Excellent agreement with the previous data (Kratz *et al.*) and evaluations (ENDF/B-VIII.0).
- Procurement of the neutron energy spectrum of  $^{86}\text{As}$

# THE END